

Influence of thermo-mechanical properties of polymer matrices on the thermal conductivity of adhesives for microelectronic packaging*

J. FELBA, T. FAŁAT**, A. WYMYSŁOWSKI

Faculty of Microsystem Electronics and Photonics, Wrocław University of Technology,
ul. Janiszewskiego 11/17, 50-372 Wrocław, Poland

Thermally conductive adhesives are among major concerns of contemporary microelectronics. The main goal of ongoing research is to improve the thermal conductivity of these composites by using a proper filler material and the best shape and size of filler particles. In this work, it has been proven by numerical simulation that the polymer matrix may also play a crucial role, as the contact area between filler particles depends on the stresses that occur due to the shrinkage of the resin during curing. It has been observed that the resins relax with time. The time until the fully relaxed state is reached strongly depends on the temperature at which the system operates. In the considered case, the contact pressure is fully relaxed when it decreases from the initial value of 0.73 GPa to 0.03 GPa. When the temperature is 70 °C, the contact pressure becomes fully relaxed after 10 seconds, but when it is lower than 40 °C, the relaxation is completed after about 10^9 seconds (more than 30 years!). After the relaxation of contact pressure, the thermal conductivity drops by approximately 50% of the initial thermal conductivity of the non-relaxed structure.

Key words: *thermal conductivity; thermally conductive adhesives; polymer matrix; microelectronic packaging*

1. Introduction

The continuous miniaturization of electronic devices and components depends on ever higher packaging densities. This introduces problems with heat transport and heat dissipation, which at present are becoming crucial issues and require the application of materials with high thermal conductivity and novel packaging methods. Thermally conductive adhesives (TCA) seem to be among the most attractive materials for this purpose.

*Presented at the joint events 1st Workshop "Synthesis and Analysis of Nanomaterials and Nanostructures" and 3rd Czech-Silesian-Saxony Mechanics Colloquium, Wrocław, Poland, 21–22 November, 2005.

**Corresponding author, e-mail: tomasz.falat@pwr.wroc.pl

Conductive adhesives consist of a polymer base material matrix and a metal filler dispersed randomly. Conduction is provided by metal additives, and high conductivity requires high metallic content, considerably above the percolation threshold. It is believed that at this concentration all conductive particles contact each other and form a three-dimensional network. The expected conductivity is obtained after the curing process due to a better contact between filler particles, resulting from the shrinkage of the polymer matrix. Thermal conductivity is limited by the so-called thermal contact resistance between filler particles. The contact thermal resistance depends on both the material properties and geometric parameters of the contact areas between particles. The geometric parameters are related to the contact pressure within the contact area. TCAs are typically formulated analogously to electrically conductive adhesives with conductive particles (usually silver flakes with average particle dimensions of several micrometers) and a polymer matrix (usually a thermosetting epoxy resin). The thermal conductivity of such composites reaches values lower than 3 W/(m·K) [1]. The conductive particles in adhesives are responsible for thermal contacts, while the polymer matrix mainly provides the mechanical interconnections.

2. The role of the adhesive filler material

The filler material is responsible for heat transport. Thermal conductivity of the bulk material is given by the equation

$$\lambda = \frac{1}{3} (c_e v_e L_e + c_{ph} v_{ph} L_{ph}) = \lambda_e + \lambda_{ph} \quad (1)$$

where c_e and c_{ph} are the heat capacities per unit volume [J/(m³·K)] of electrons and phonons, respectively, v_e and v_{ph} are their root-mean-square velocities, and L_e and L_{ph} are their mean free paths. Since λ_e is the dominant part of the thermal conductivity of metals, one can roughly assume that

$$\lambda = \lambda_e \quad (2)$$

In the case of copper at room temperature, $\lambda_e = 380$ W/(m·K) and $\lambda_{ph} = 21$ W/(m·K).

Generally, because of their relatively low cost, pure metals such as copper or silver are the best candidates for TCA fillers. There are also materials with much higher thermal conductivities reaching 2000 W/(m·K) for synthetic diamond and up to 3000 W/(m·K) for carbon nanotubes. Carbon nanotubes consist of graphite sheets wrapped into hollow cylinders with the diameters as small as 1 nm and lengths in the micrometer range. Their unique mechanical and thermal properties make them ideal fillers in the development of a new generation of composite materials for, among others, microelectronic packaging. For certain applications, high thermal conductivity and electrical insulating properties are needed. Aluminium nitride particles (7 μ m) and whisk-

ers (250 μm) or silicon carbide whiskers could be used as fillers in TCAs for such purposes. [2]

Generally, the filler particles used in thermally conductive adhesives occur in many different shapes, such as spheres, flakes, whiskers, tubes, fibres, etc., and their dimensions vary from micro- to nanometers.

3. The role of contacts between filler particles

Tests with TCAs containing different filler materials show that there is no simple relationship between the conductivities of the bulk material and composite. For example, synthetic diamond powder as the filler reveals a low value of TCA thermal conductivity compared to silver flakes [3]. This is believed to be due to the presence of nitrogen and other impurities in the synthetic diamond, but generally small contact areas between filler particles significantly reduce the thermal conductivity of the adhesive. If contact members are in the form of perfect hard balls, they touch each other at one point (the contact point *A* in Fig. 1). In fact, this point turns into a small area, since the contact materials are deformable.

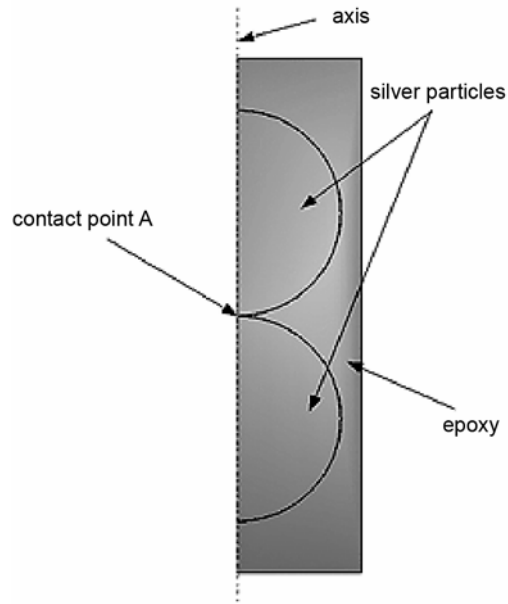


Fig. 1. 2D axis-symmetric model of silver-filled TCA

The thermal contact resistance between particles can be lowered by using mixed filler materials that differ in particle sizes. Composites containing silver particles and nanoparticles improve thermal conductivity even by the factor of 2.55 [4]. Furthermore, the thermal conductivity of TCAs can be improved by using fillers with different particle shapes (e.g., spheres + whiskers) [2, 5]. Both of these techniques are

costly and require a lot of experiments to be performed with various material contents and configurations in order to obtain optimal results.

Therefore, it is worth asking: how does the contact state between particles affect the thermal conductivity of TCA? In order to test this, a numerical modelling of silver-filled TCA was performed. The numerical model was simplified by some assumptions: identical, spherical silver particles were used as the filler, a closely packed (HCP or FCC crystal equivalent) 3D structure was analysed as the unit cell (see Fig. 2), the particles touch each other, and the contact properties were described by contact areas (impurities and roughness were neglected). The closely packed structure was assumed as a consequence of the maximal possible packing efficiency ($V_{\text{filler}}/V_{\text{total}} = 74.05\%$) for the 3D spherical particles.

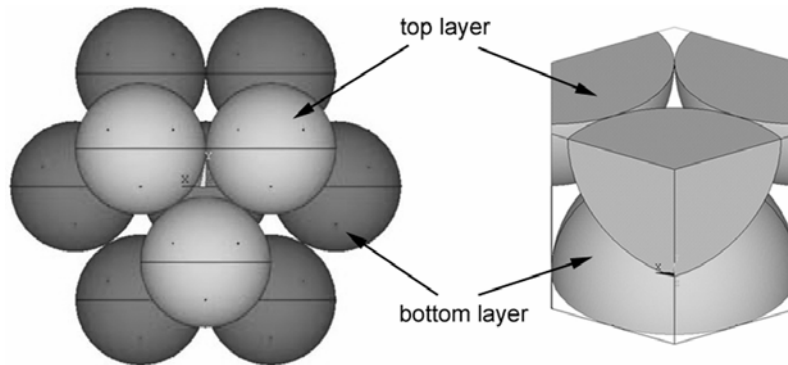


Fig. 2. Closely packed structure (left) and the analysed unit cell (right)

The unit cell shown in Fig. 3 was analysed with ANSYS 8.0 commercial FEM software. Two different contact area radii were taken into account and represented by the r/R relation, where r is the contact area radius and R is the particle radius. The results of the simulation are collected in Table 1.

Table 1. Results of numerical simulation

r/R	λ [W/(m·K)]
0.05	49.12
0.02	26.46

As shown in Table 1, the contact area between the filler particles has a strong influence on the thermal conductivity of TCA. This area depends on the stress between the particles, which occurs due to the shrinkage of the resin during curing. Calculating this stress is quite complex because of its temporal relaxation due to the viscoelastic behaviour of the resin.

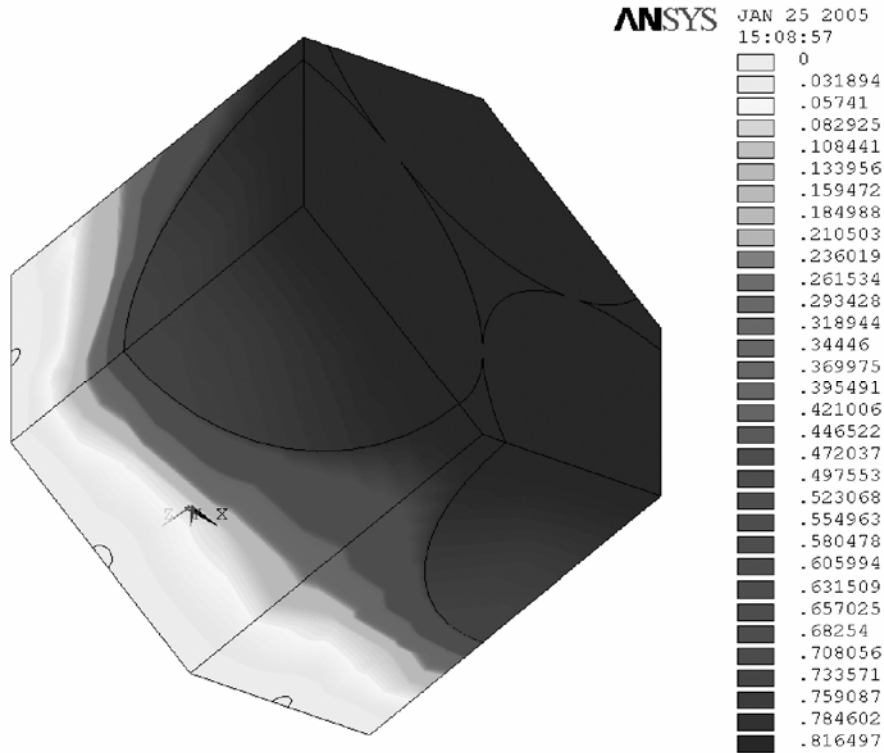


Fig. 3. The unit cell analysed by ANSYS 8.0

4. The role of the polymer matrix

An adhesive matrix is used to form mechanical bonds at interconnections. Polymeric materials have thermal conductivities about 2000 times lower than silver or copper. Thermal conductivities of all polymeric materials, epoxy or other types, thermoset or thermoplastic, range from 0.2 to 0.3 W/(m·K). Nevertheless, the thermo-mechanical properties of polymer matrices may strongly influence the thermal conductivity of adhesives for microelectronic packaging.

4.1. Viscoelasticity

The general linear viscoelastic equation is the basic equation for modelling the development of viscoelastic stresses (σ_{ij}) as a function of temperature and loading time in fully cured polymer materials:

$$\sigma_{ij}(t, T) = \int_{-\infty}^t \{ 2G(t-s, T) \dot{\epsilon}_{ij}^d + K(t-s, T) \dot{\epsilon}_V^{\text{eff}} \} ds \quad (3)$$

where G and K denote the shear and bulk relaxation moduli, respectively (they are time- (t) and temperature- (T) dependent), and $\dot{\varepsilon}_V^{\text{eff}}$ is the effective strain contribution.

Shear and bulk moduli also depend on the conversion level (degree of cure, α). Therefore, the viscoelastic stress described by Eq. (3) can be written as:

$$\sigma_{ij}(t, T, \alpha) = \int_{-\infty}^t \left\{ 2G(t-s, T, \alpha) \dot{\varepsilon}_{ij}^d + K(t-s, T, \alpha) \dot{\varepsilon}_V^{\text{eff}} \right\} ds \quad (4)$$

and $\dot{\varepsilon}_V^{\text{eff}}$ consists of mechanical, thermal, and cure shrinkage parts [6, 7]:

$$\varepsilon_V^{\text{eff}} = \varepsilon_V^{\text{mech}} - \varepsilon_V^{\text{cure}} - \varepsilon_V^T, \quad \varepsilon_V^T = 3\beta_L^{g,r}(T - T_{\text{ref}}) \quad \varepsilon_V^{\text{cure}} = -3\gamma_L(\alpha - \alpha_{\text{ref}}) \quad (5)$$

where β_L^g and β_L^r are the linear coefficients of thermal expansion (CTE) measured below the glass transition temperature T_g (glassy region) and above T_g (rubbery region), respectively, and γ_L is the linear cure shrinkage. The change of the modulus during curing can be explained by the change in the molecular structure of the matrix. Since cure-dependent viscoelasticity is not implemented in commercial FEM software such as ANSYS 8.0 or ABAQUS 6.5, only the results of measurements for fully cured materials were used and the cure dependence of the relaxation modulus was neglected.

If the time is relatively short ($t \rightarrow 0$), shear and bulk relaxation moduli are treated as instantaneous shear and bulk moduli G_0 and K_0 , respectively, and they can be determined from the values of the instantaneous (obtained from the high-rate tests) elastic (Young) modulus E_0 and Poisson's ratio ν_0 :

$$G_0 = \frac{E_0}{2(1+\nu_0)} \quad \text{and} \quad K_0 = \frac{E_0}{3(1-2\nu_0)} \quad (6)$$

Poisson's ratio is often assumed to be time-independent in viscoelastic materials, therefore Eq. (6) can be used for the whole time scale of the shear, bulk, and elastic relaxations up to the point when strains are small. The advantage of such an approach is that when modelling the behaviour of viscoelastic materials only one modulus needs to be measured (e.g., the shear relaxation modulus) and the other can be calculated from Eq. (6).

The effect of temperature in Eq. (3) is usually not included as $G(t, T)$, but as $G(t_{\text{red}}(T))$, where t_{red} is the so-called reduced time scale and $G(t_{\text{red}})$ is referred to as the master curve. The reduced time scale is defined as

$$t_{\text{red}} \equiv \int_0^t a_T dt \quad (7)$$

where a_T is the temperature-dependent shift factor, which can be described by the WLF (Williams, Landel, Ferry) equation

$$a_T = \exp \left\{ -\frac{C_1 (T - T_{\text{ref}})}{C_2 + T - T_{\text{ref}}} \right\} \quad (8)$$

T_{ref} is the reference temperature, and C_1 and C_2 are material parameters. The reduced time scale t_{red} can be replaced by the reduced frequency scale $f_{\text{red}} = a_T f$.

4.2. Experimental procedures

The standard way of measuring dynamic changes of the mechanical parameters of shear modulus (for polymeric materials in particular) is a continuous monitoring of the thermo-mechanical properties from the liquid to the fully cured state by applying the liquid compound (e.g. resin + hardener) in small gaps between parallel plates of the shear clamps of a dynamic mechanical analyzer (DMA). The samples are subject to a series of sinusoidal strains or stresses at different frequencies (a frequency sweep). The temperature is then increased by 5–10 °C and another frequency sweep is applied. This procedure is repeated from about 80 °C below the glass transition temperature (T_g) to about 80 °C above it. Far below the glass transition temperature the modulus data (stress amplitude divided by strain amplitude) is frequency independent. This modulus is called the glassy modulus. Far above the glass transition temperature, the material either melts, as is typical of thermoplasts, or displays a nonzero, frequency-independent rubbery modulus of thermosets. In between, in the so-called viscoelastic region, the modulus is frequency-dependent and lies between the glassy and the rubbery values. It is customary to shift the individual modulus vs. frequency curves along the logarithmic frequency axis until they overlap and form a master curve. The shift (a_T) is different for each temperature. The master curve, together with this shift factor, completely describe the temperature and frequency-dependent modulus data and can even be used to predict the mechanical behaviour at time scales and temperatures different from those of the test conditions [8].

4.3. Numerical approach

To study the contact pressure occurring between the filler particles due to the cure shrinkage of the polymer matrix and its influence on thermal conductivity, the model shown in Fig. 1 was implemented by ABAQUS v.6.5 FEM software [9]. It is the 2D axis-symmetric model, which consists of two identical spherical silver particles surrounded by cylindrically shaped epoxy resin. The volume fraction of filler was about 23%. The particles touch each other at one point at the beginning of the simulation. The contact pressure and its change in time after curing at different temperatures were monitored at the contact point A .

Silver (as the filler) is considered to be a linear elastic material with the elastic modulus $E = 76$ GPa and the Poisson's ratio $\nu = 0.37$. The thermal conductivity of silver is 423 W/(m·K).

The tested epoxy resin was delivered by Amepox Microelectronics, Poland. The linear reaction cure shrinkage was assumed at the level of 1×10^{-2} (volume shrinkage $\approx 3 \times 10^{-2}$). To determine the viscoelastic properties of the fully cured epoxy sample, dynamical mechanical thermal analysis (DMTA) was performed. The DMTA measurements were conducted using a TA Instruments ARES rheometer (the tool: torsion pendular; geometry: rectangle). The dynamic mechanical shear tests were performed to obtain the storage and loss relaxation moduli. The tests were performed in the Fraunhofer Institut für Fertigungstechnik und Angewandte Materialforschung, Bremen, Germany.

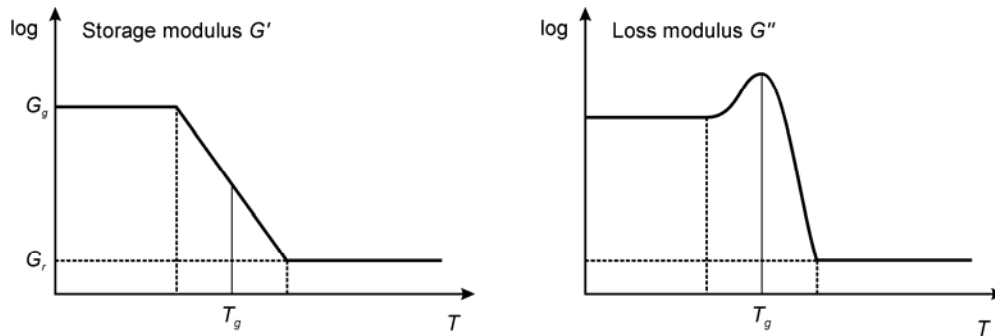


Fig. 4. The storage (G') and loss (G'') shear moduli for the fully cured material vs. temperature

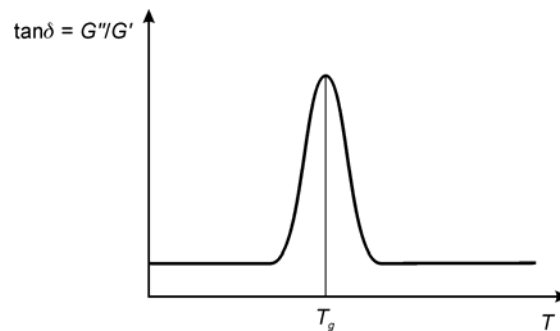
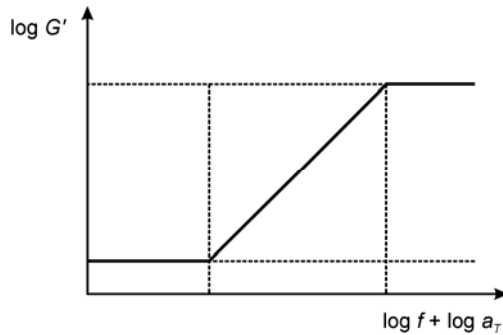
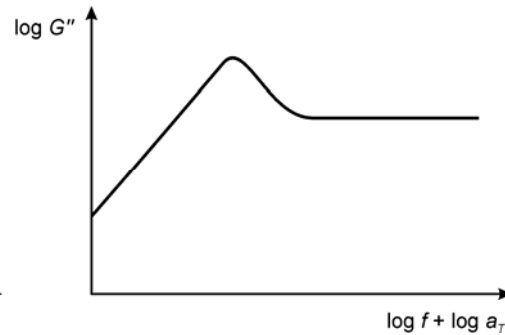


Fig. 5. The loss angle $\tan \delta = G''/G'$ vs. temperature

Figure 4 shows an example of the storage (G') and loss (G'') moduli as functions of temperature. In Figure 5, an example of the temperature dependence of the loss angle $\tan \delta = G''/G'$ is shown. It is possible to deduce the glass transition temperature T_g from these data. The glass transition temperature does not show a sharp transition from one state into another but a gradual change. There appears to be no consensus in the literature on its precise definition [10]. Therefore, the two following criteria are applied for the measurement of T_g : the peak in the loss modulus G'' vs. T and the peak in the loss angle $\tan \delta$ vs. T . The measured T_g values were as follows: $T_g = 55$ °C (for the peak in the loss modulus G'') and $T_g = 68$ °C (for the peak in the loss angle $\tan \delta$).

By measuring the storage modulus G' and loss modulus G'' as a function of frequency at various temperatures, it is possible to construct master curves for the storage and loss moduli. Examples of the master curves are shown in Figs. 6 and 7.

Fig. 6. Master curve of the storage modulus G' Fig. 7. Master curve of the loss modulus G''

When constructing the master curves, the shift factor a_T has to be evaluated (see Eq. (8)) by estimating the values of the WLF equation parameters. The parameters of the WLF equation for the considered epoxies are collected in Table 2.

The simulation procedure was divided into two steps. In the first step, a steady state analysis was performed to simulate the shrinkage caused by curing the epoxy and to monitor the initial contact pressure between silver particles. In this step, the epoxy resin was treated as an elastic material and the cure dependence and viscoelastic properties were neglected. Since the cure shrinkage is not implemented in ABAQUS v.6.5, it was simulated by using thermal expansion features. The coefficient of thermal expansion (CTE) was fixed at $1 \times 10^{-4} \text{ K}^{-1}$ and the temperature was lowered from the initially elevated temperature ($T_0 + 100 \text{ }^\circ\text{C}$) to the temperature at which the second step was performed (T_0). After this procedure, it was possible to obtain a linear shrinkage of 1×10^{-2} . In the second step, transient analysis was performed and various temperatures (T_0 changes from $40 \text{ }^\circ\text{C}$ to $70 \text{ }^\circ\text{C}$) were applied to observe the temperature dependence of the contact pressure relaxation.

Table 2. Estimated parameters for the WLF equation (Eq. (8))

Parameter	Estimate
T_{ref}	$60 \text{ }^\circ\text{C}$
C_1	17.66
C_2	$80.58 \text{ }^\circ\text{C}$

The results of the simulations, i.e. the contact pressures between particles vs. time for different temperatures, are shown in Fig. 8.

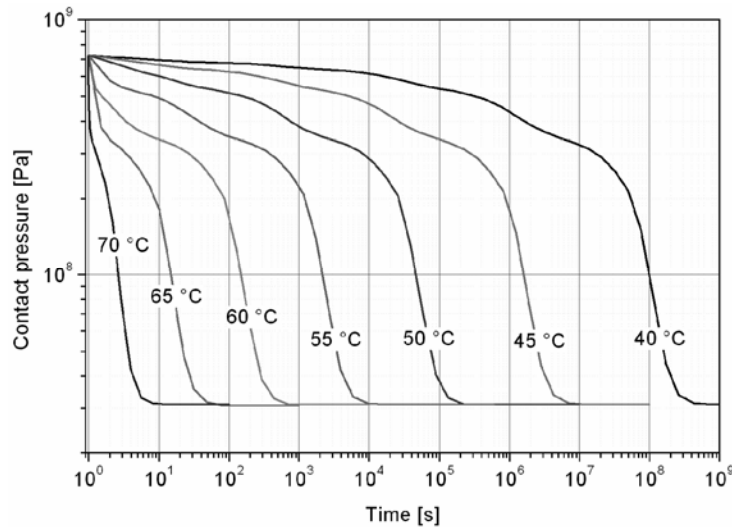


Fig. 8. The results of simulation—contact pressure between the filler particles vs. time for various temperatures

The contact pressure occurring between filler particles due to the cure shrinkage relaxes within time. The time needed to reach the fully relaxed state strongly depends on the working temperature of the system. In the considered case, the contact pressure is fully relaxed when it decreases from an initial value of 0.73 GPa to 0.03 GPa, as shown in Fig. 8. When the temperature is 70 °C, the contact pressure becomes fully relaxed after 10 seconds, but when it is lower (e.g. 40 °C) the full relaxation state is reached after about 10^9 seconds (more than 30 years!).

The thermal conductivities of the tested structures have been calculated (using FEM) before and after relaxation. After the relaxation of the contact pressure, the thermal conductivity drops to around 50% (0.484) of its initial value for the unrelaxed structure.

5. Conclusions

Thermally conductive adhesives consist of a polymer base matrix and a filler, which is mainly responsible for thermal conductivity. Silver in the form of flakes with average particle dimensions of several micrometers is typically used as the filler. Pure metals with thermal conductivity about 400 W/(m·K) can be replaced by much more conductive materials such as synthetic diamond (2000 W/(m·K)) or carbon nanotubes (up to 3000 W/(m·K)). Nevertheless, there is a lack of reports concerning the significant influence of those materials on the thermal conductivity of adhesives for micro-electronic packaging. The main reason for the huge differences between the thermal conductivities of bulk materials and composites is due to small contact areas between filler particles. In the case of identical, spherically shaped silver particles, the numerically calculated value of thermal conductivity reaches 26.46 W/(m·K). The particles

are closely packed (HCP or FCC crystal equivalent) with the ratio of particles radius to contact area radius being 0.02. Certainly, such an ideally shaped and closely packed filler is an oversimplification, but it does indicate theoretical limits.

As calculated using the model presented above, the contact area between filler particles has a strong influence on the thermal conductivity of the adhesive. This area depends on the stress between particles, which occurs due to resin shrinkage during curing, indicating that the role of the polymer matrix is more important than only forming mechanical bonds at interconnections. Calculating such a stress is quite complex because of its temporal relaxation due to the viscoelastic behaviour of the resin.

In the simulation procedure, transient analysis was performed in order to observe the temperature dependence of contact pressure relaxation between filler particles. The time needed for it to reach the fully relaxed state strongly depends on the temperature at which the system operates. The contact pressure relaxation time changes from 10 seconds at 70 °C to about 10^9 seconds (more than 30 years) at 40 °C. After relaxation of the contact pressure, the thermal conductivity drops to around 50% (0.484) of its initial value for the unrelaxed structure.

Acknowledgements

Authors would like to thank Mr. Andrzej Moscicki from AMEPOX Microelectronics, Poland for supplying the epoxy resin and Ms. Jana Kolbe from IFAM Fraunhofer Institut fuer Fertigungstechnik und Angewandte Materialforschung, Klebetechnik und Oberflaechen, Germany for the measurements.

References

- [1] FALAT T., FELBA J., WYMYSŁOWSKI A., Proc. of 28th International Conference of IMAPS Poland Chapter, Wrocław, 2004, p. 219.
- [2] XU Y., CHUNG D.D.L., MROZ C., Composites A: Appl. Sci. Manufacturing, 32 (2001), 1749.
- [3] BOLGER J.C., *Prediction and measurement of thermal conductivity of diamond filled adhesives*, IEEE Publ. No 0569-5503/92/000-0219, 1992.
- [4] UKITA Y., TATEYAMA K., SEGAWA M., TOJO Y., GOTOH H., OOSAKO K., Proc. of IMAPS2004, Long Beach, USA, 2004, WA71.
- [5] LI H., JACOB K.I., WONG C.P., IEEE Trans. Adv. Packaging, 26 (2003), 25.
- [6] JANSEN K.M.B., WANG L., YANG D.G., VAN 'T HOF C., ERNST L.J., BRESSERS H.J.L., ZHANG G.Q., Proc. of IEEE 2004 Electronic Components and Technology Conference, Las Vegas, Nevada, 2004, p. 890.
- [7] JANSEN K.M.B., WANG L., VAN 'T HOF C., ERNST L.J., BRESSERS H.J.L., ZHANG G.Q., Proc. 5th Int. Conf. on Thermal and Mechanical Simulation and Experiments in Micro-electronics and Micro-Systems EuroSimE, Brussels, 2004, p. 581.
- [8] MILOSHEVA B.V., JANSEN K.M.B., JANSSEN J.H.J., BRESSERS H.J.L., ERNST L.J., 6th. Int. Conf. on Thermal, Mechanical and Multiphysics Simulation and Experiments in Micro-Electronics and Micro-Systems, EuroSimE, Berlin, 2005, p. 462.
- [9] FALAT T., WYMYSŁOWSKI K., KOLBE J., Proc. of 5th International IEEE Conference on Polymers and Adhesives in Microelectronics and Photonics Polytronic2005, Wrocław, Poland, 2005, p. 180.
- [10] MEUWISSEN M.H.H., DE BOER H.A., STEIJVERS H.L.A.H., SCHREURS P.J.G., GEERS M.G.D., *Microelectronics Reliability*, 44 (2004), 1985.

Received 21 February 2006

Revised 28 May 2006

